Materials Research Express

PAPER • **OPEN ACCESS**

Synthesis and physical characterization of magnetron sputtered Graphene-CdS bilayer

To cite this article: Harshita Trivedi *et al* 2021 *Mater. Res. Express* **8** 055003

Materials Research Express

OPEN ACCESS

RECEIVED
25 February 2021

REVISED
7 May 2021

ACCEPTED FOR PUBLICATION
11 May 2021

PUBLISHED
19 May 2021

PAPER

Synthesis and physical characterization of magnetron sputtered Graphene-CdS bilayer

Harshita Trivedi[1], **Hanieh Shafaghi**[2], **Naresh Shagya**[3], **Jayeeta Lahiri**[3,4], **Zohreh Ghorannevis**[2,*] and **Avanish S Parmar**[1,*]

[1] Department of Physics, Indian Institute of Technology (BHU), Varanasi, India
[2] Department of Physics, Karaj Branch, Islamic Azad University, Karaj, Iran
[3] School of Physics, University of Hyderabad, Hyderabad 500046, India
[4] Department of Physics, Banaras Hindu University, Varanasi, India
[*] Authors to whom any correspondence should be addressed.

E-mail: ghoranneviszohreh@gmail.com and asparmar.phy@itbhu.ac.in

Keywords: Graphene-CdS, hybrid material, graphene sheet, RF Sputtering method

Abstract

CdS/Graphene Nano composites have been extetinsively investigated in the field of basic industrial research and electronic device applications because of their unique physical, chemical properties and photo stability under visible-light irradiation. In this study, we explore the electrical properties of Cadmium sulfide with the addition of graphene. CdS/Graphene hybrid was fabricated by simple RF magnetron sputtering method using CdS as a sputtering source. The hybrid material formation and structural properties of Graphene, CdS, CdS/Graphene have been discussed using XRD, FTIR, Raman, and UV–vis spectroscopy techniques. Herein, we present a facile and efficient method for hybridization of CdS Nano-sphere with graphene Nano sheet and subsequent investigation of enhancement of current of the hybrid material. Field emission scanning electron microscopy (FESEM) micrographs reveal the formation of CdS nanospheres and homogeneous scattering on the surface of graphene sheets. The UV absorption spectrum of CdS/Graphene hybrid presented a red-shifted. The enhancement in the current of CdS/Graphene hybrid has been observed due to the generation of electron-hole pairs. Also, current-voltage (I-V) characteristics of an as-grown thin film of the hybrid are conducted using 4-point probe measurement and revealed their semiconducting nature with a drastic enhancement of electrical conductivity.

1. Introduction

Semiconductor nanocrystals have received great interest in basic research and industrial development due to their special electronic and physical properties [1, 2]. Various organic and inorganic broadband semiconductor materials such as ZnS, ZnO, TiO_2, GaN, CdS, quantum dots of graphene, and its compound have been investigated in various electronic device applications due to their fascinating properties [3–8]. In particular, II-VI semiconductor-multilayer structures have gained much attention as being suitable for various device applications [9]. Among these semiconductors, cadmium sulfide (CdS) (AII-BVI compounds) shows excellent applicability in various fields (photovoltaic devices, light-emitting diode, thin-film transistors, and photocatalysts) due to its wide energy bandgap i.e. ~2.42 eV, emission tunability, good transparency, n-type conductivity, excessive stability, excellent extinction coefficient and high dipole moment [10–13]. However, the limitations associated with cadmium-based semiconductors are poor surface area and speedy recombination rate of charge carrier generated throughout photo excitation method [14–19]. The simple and effective technique to decrease fast recombination method is the coating of environment-friendly electron-transport material, such as conductive polymer thin films, carbon nanotubes (CNTs), Graphene [17, 20–23].

Among others, Graphene received attention due to its great chemical and physical properties [24–27]. Because of various beneficial characteristics, Graphene is the most suitable support for developing a hybrid

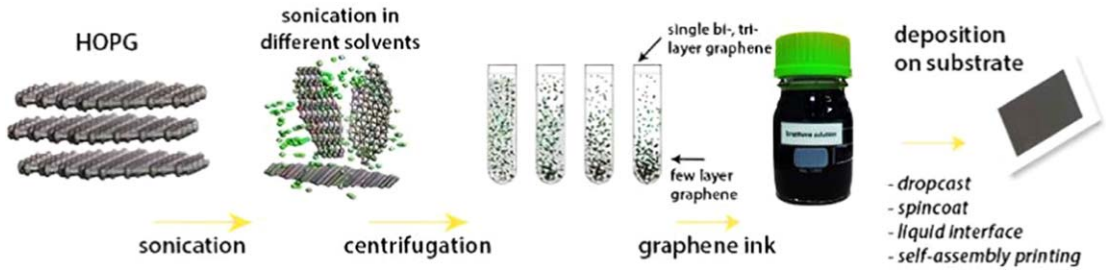

Figure 1. Graphene dispersion stages on the substrate.

Figure 2. Address layer of cadmium sulfide sample grown on graphene.

material with improved features [28–30]. It was reported earlier that graphene played an important role in device application due to close conduction distance and extensive transmission efficiency excessive transmission performance [31–33].

Up to now a survey of the literature shows that various deposition techniques have been developed for CdS thin films deposition among which pulsed laser deposition (PLD) [34], Chemical bath deposition [35, 36], Molecular beam epitaxy (MBE) [37, 38], Spray Pyrolysis [39, 40], Sputtering [41–43] and Thermal evaporation [44, 45]. Herein, a series of CdS/Graphene hybrid was prepared via RF sputtering method to obtain optimum experimental conditions to enhance the physical properties. RF sputtering method is a useful technique used in CdS thin film deposition permitting a great control of film consistency, controlled morphology, contamination-free environment, and thickness over large area substrates than other methods [46–48]. The kinetic energy of atoms produced and their substrate interactions determine thin film growth in RF sputtering. The kinetics of atoms incident on the substrate are influenced by sputtering parameters such as deposition pressure, time, sputtering strength, and substrate temperature, which then affect the growth mechanism, resulting in improving the overall performance of CdS thin films.

However, in terms of the electric current, optimization of CdS for exceptional amounts of Graphene has not been reported. The synthesized thin film was characterized by relevant basic and performance tests essential and execution tests. Additionally, a detailed study of the physical properties of CdS/Si, Graphene/Si, CdS/Graphene/Si thin films are undertaken to optimize structural, electrical, and surface topographical properties for CdS thin film for various device application like as an absorber layer of solar cells. The hybrid exhibit great potential in various field of electronic devices having an overall performance having large sensitivity, maximum quantum efficiency, and good response speed. Finally, we present our conclusion and perspectives.

2. Methods and characterization

2.1. Fabrication of film

CdS/Graphene hybrid material thin film was deposited via RF magnetron sputtering under controlled growth conditions with RF power 150 W on n-type (422) single crystal silicon wafers substrates at room temperature under high vacuum ($2 \sim 10^{-6}$ Torr). The resistivity and thickness of silicon wafers were (300 ± 20 μm) and (3000 to 6000 Ωm), respectively. Graphene nanoplates were dispersed in ethanol by sonication for 20 min to give graphene ink with an approximate ratio of 5 mg l^{-1} as shown in figure 1.

Graphene Nanoplates with 99.5 wt% purity and volume resistivity 4×10^{-4} Ω.cm used as a growing layer on silicon. We used a solid compact plate of CdS target. The dimension of silicon substrates was 1 cm $\times$ 1 cm. Substrates were ultrasonically cleaned first using alcohol for 5 min then acetone for 10 min. The substrates have been organized with a standard cleaning technique utilizing natural organic solvents earlier that being etched in HCl for 30 s [49], rinsed for 10 min with de-ionized water, dried with nitrogen fuel to cast off surface contamination, and fixed on the substrate holder. The CdS-nanoparticles decorated graphene Nanosheets (CdS/Graphene on the silicon wafer) and on the silicon substrate were prepared by a Magnetron Sputtering with the RF power of 150 W as shown in figure 2.

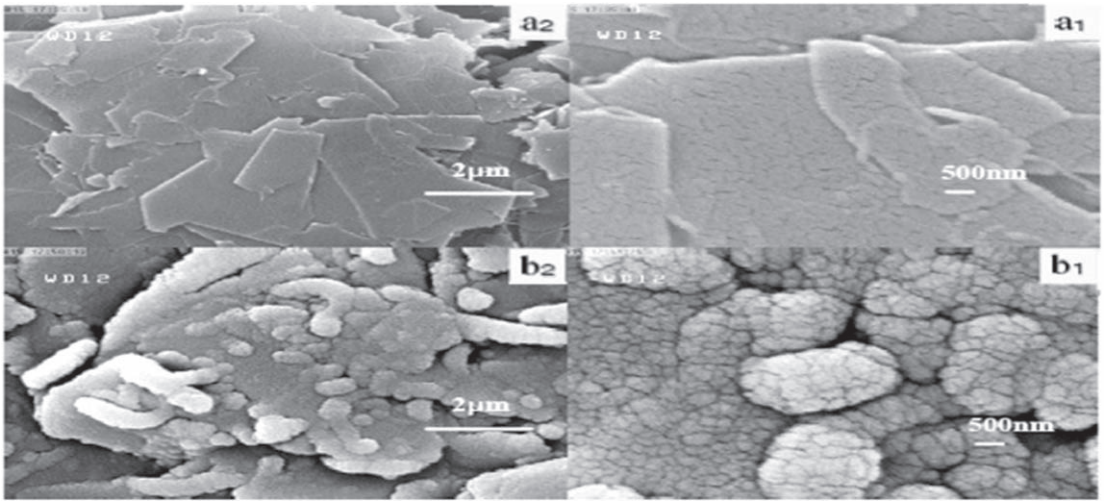

Figure 3. FESEM images of (a_2,a_1) Graphene/Si, (b_2,b_1) Graphene/CdS/Si.

Table 1. The table of experiment conditions and parameters.

Parameters	Test conditions
Graphene Density	5 mg ml^{-1}
Solvents	Ethanol (merck)
Sonication Time	20 min
Substrate temp.	°40 + 5°C

The basic parameters like base pressure and deposition pressure have been set as10^{-6} Torr and 2×10^{-2} Torr, respectively. The separation between the target and the substrate was ~7 cm for synthesizing uniform consistent thin films, substrates had been kept rotating all through the sputtering process. And the deposition time was set to 20 min (table 1).

2.2. Characterization

The sample was characterized by several techniques like UV–vis FTIR, Raman spectra, and I-V characteristics. The morphology of Graphene/Si, CdS/Si, and CdS/Graphene/Si, and films were investigated under a Field emission scanning electron microscope using a HITACHI S-4160. For structural analysis of Graphene/Si, CdS/Si, and CdS/Graphene/Si thin films were carried out which was equipped focused by X-ray diffraction (Philips Xpert, with Cu-Ka radiation ($\lambda = 0.15418$ nm)). Further, a dual-beam UV–vis spectrophotometer (Cary 500 UV/VIS/NIR spectrophotometer) was used utilized to investigate the absorption properties and transparency over the spectral region of 200–800 nm. FTIR spectroscopy was used to investigate with an accuracy of 0.1 nm in the range of UV/VIS and 0.4 nm in the range of NIR and wavelength ranging from 175 to 3300 nm using Thermo Nicolet Nexus 870 spectrometer. Current-Voltage (I-V) measurements were also performed on different samples. The voltage applied to the specimen from the stabilized DC power supply was increased from −1 V to +1 V. The voltage connected to the sample and the current flowing through it was measured using electrometers of type (Keithley-2361). Synthesized samples have been recorded using Thermo/Nicolet FT-Raman 960, having a spectral range of 400 cm^{-1} to 4000 cm^{-1} with a He/Ne laser (excitation wavelength of 633 nm). The electrical resistivity measurements on samples were determined by the four-point probe.

3. Results and discussion

3.1. Surface morphology

Figure 3 demonstrates the FESEM micrographs of Graphene/Si and CdS/Graphene/Si hybrid material. As seen in figures 3a_1 and a_2 graphene show a 2D sheet-like surface, which plays an important role as a supporting material in CdS growth. As seen in figures 3b_1 and b_2 hybrid show that CdS particle randomly stacked together had a uniform distribution over graphene sheets. Hybrid indicates an appropriate interfacial interaction between CdS particle and graphene sheets. The as-deposited thin films exhibits irregular grains and bubbles

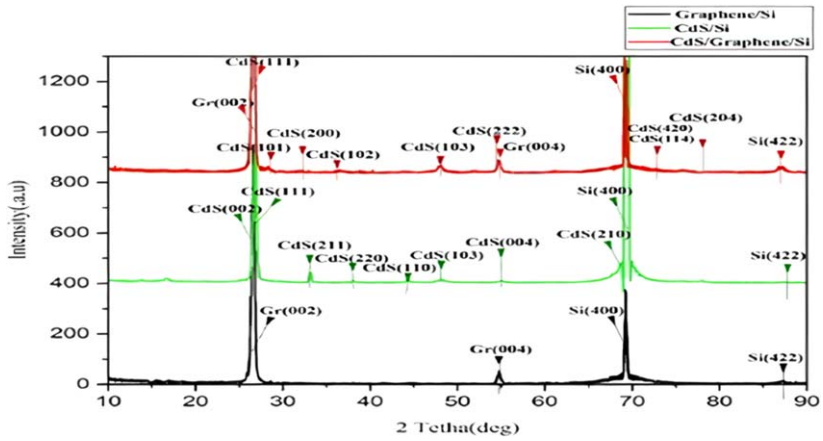

Figure 4. XRD results of pristine graphene, CdS/Graphene nanocomposite, and pure CdS NPs.

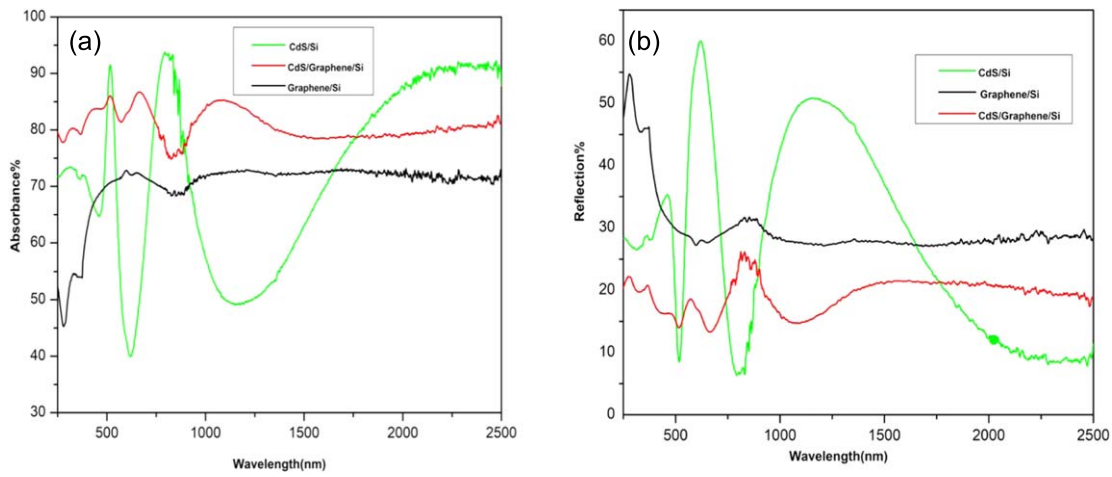

Figure 5. (a) UV–vis spectra (b) UV–vis reflectance spectra graphene/Si, CdS/Si, CdS/graphene/Si hybrid.

exhibits in the surface because of their crystalline structure. Sheets of Graphene are curled and grooved and the surface morphology of CdS particles shows spherical morphology with less aggregation and a smaller diameter, which offers a large surface area that benefits various electronic device applications [50].

3.2. X-ray diffraction analysis

To study various phases and crystallinity of synthesized material, XRD was performed using Philips Xpert, with Cu-Ka radiation ($\lambda = 0.15418$ nm). Figure 4 indicates the XRD pattern of the graphene, pure CdS, and CdS/Graphene hybrid. The diffraction peaks of the graphene sheet at $2\theta \sim 26^\circ$ and 54° matched properly with the hexagonal crystal structure of graphene and were indexed as (002) and (004) facets, respectively [51, 52]. The peaks at 2θ values of 26.51, 38.51, 43.71, 47.81, and 54.81 can be ascribed to the (002), (220), (110), (103) and (004) crystal planes of hexagonal CdS, respectively [53]. Additionally, all the XRD peaks of the pure CdS coordinate similar to CdS with the hexagonal crystal structure and were identified as the (002), (220), (110), (103), and (004) planes of the hexagonal structure [44].

The X-Ray diffraction pattern sample of the CdS/Graphene hybrid appears to be a simple mixture of the reflection pattern of Graphene and natural CdS, where no significant modifications were observed in the relative intensity of every peak. The strongest peak, at $2\theta \sim 26^\circ$, is believed to correspond to each carbon (002) and CdS (002), which shows almost equal to identical positions. Synthesized hybrid material indicates decrease intensities than those for natural CdS. This would be due to the graphene wrapped across the surface of the CdS particles. Hybrid material exhibits comparable diffraction peaks with pure CdS particles, while no diffraction peak of graphene was examined because the regular stack of graphene sheets is destroyed by the intercalation of CdS particles [54]. This indicates out the formation of a new phase throughout the hybrid formation.

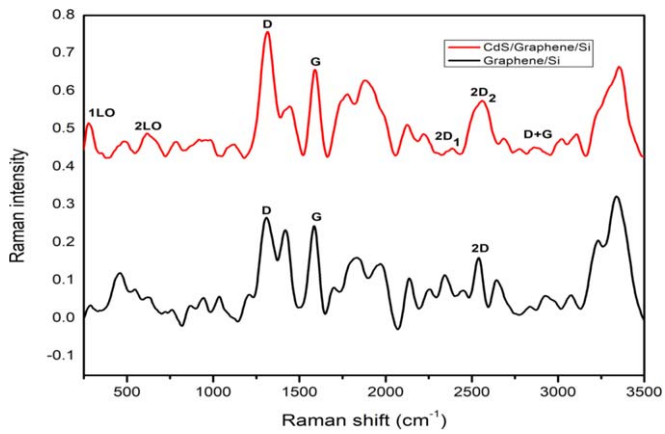

Figure 6. Raman spectra of (a) graphene and (b) CdS/Graphene hybrid material.

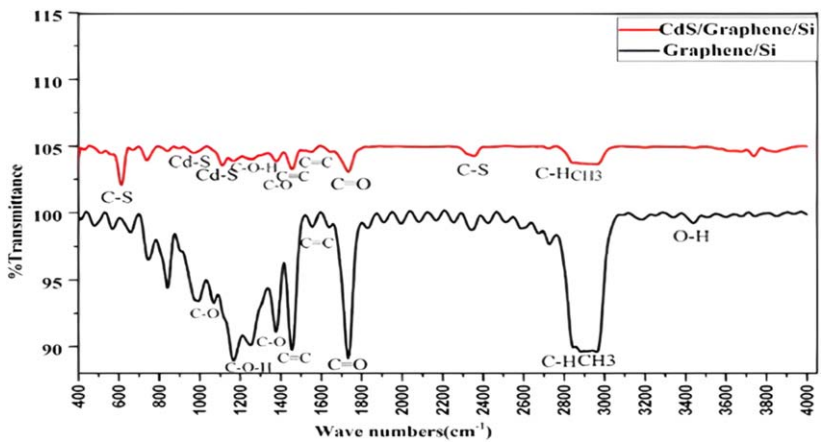

Figure 7. FTIR spectra of graphene/Si and CdS/Graphene/Si.

3.3. UV–vis spectra

The UV–Vis of CdS, Graphene, and CdS/Graphene hybrid is demonstrated in figure 5. Figure 5(a) indicates UV light absorption at different wavelengths and figure 5(b) shows UV–Vis diffuse reflectance spectra (DRS) of pure CdS and CdS/Graphene hybrid. the absorption spectra of pure CdS at 500 nm which correspond to the bandgap of 2.48 eV using the formula (Bandgap $=$ 1240/honest) [55].

After the introduction of graphene, CdS (CdS/graphene) undergo a redshift and enhanced absorption both in the ultraviolet region and visible region. Furthermore, CdS/Graphene hybrid has a continuous absorbance band is shown in CdS/Graphene hybrid matched properly with pure CdS in the visible range from 500–900 nm compared, Which is due to graphene can improve the surface electrical charge of CdS [56]. Hence, CdS/Graphene hybrid is more efficient to utilize visible light.

3.4. Raman spectral analysis

Raman spectroscopy is a viable and non-destructive experimental method that is widely used to study structural information of carbon-based materials [57]. Figure 6, appears the Raman spectra for graphene and CdS/Graphene hybrid, respectively. The results showed the existence of G-band besides the imperfections D-band in both the samples. The G-band is ascribed in-plane vibrations of sp^2 hybridized carbon atoms. The Raman spectra of graphene sheets show D and G bands allotted to the κ-point phonons of the A_{1g} symmetry and E_{2g} phonon of the sp^2 carbon at 1353 and 1593 cm^{-1}, respectively which shifts to lower wavelength 1340 and 1577 cm^{-1} after reduction due to the formation of the CdS/Graphene hybrid. Further, the two peaks at 300 and 600 cm^{-1} have been related to the longitudinal optical (LO) phonon modes of CdS/Graphene hybrid.

Three extra characteristic peaks positioned at 1345, 1573, and 2711 cm^{-1} were discovered, which compare to D, G, and 2d peaks of graphene, respectively. 2D band appears at around 2711 cm^{-1} shows the multilayer graphene structure, which was also moreover compared by other groups [58, 59]. The 2D band is originated due to a twofold resonance transition which brought because of the generation of two phonons with inverse energy

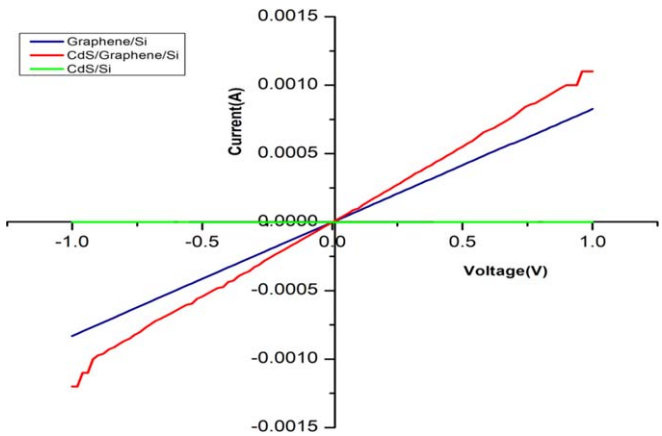

Figure 8. Current-voltage (I-V) characteristics of CdS/Si, graphene/Si and CdS/graphene/Si.

[60]. Moreover, D peak having lower intensity shows lower disorder in graphene structure [61, 62]. However, the fundamental longitudinal optical phonon mode (LO) and the first-order (1LO) phonon modes peaks of the CdS/Graphene hybrid have been decreased due to the decreasing CdS concentration in comparison to pure CdS. This also confirms the formation of the CdS/Graphene hybrid. Because cadmium sulphide has been deposited on a single-layer graphene structure, the D band intensity has increased relative to the G band, and both bands shifted to higher wavenumbers [63].

3.5. FTIR study

To understand the presence of functional groups and chemical interactions involved between different graphene and CdS functional groups, FTIR was performed using Thermo Nicolet Nexus 870 spectrometer. The FTIR spectra of (a) graphene (b) CdS/graphene hybrid materials are represented in figure 7. At 2935 cm^{-1} and 2880 cm^{-1}, The existence of two absorption band doublet is shown by pure graphene spectra corresponding to symmetric and antisymmetric stretching vibrations of the $-CH_2$ group, respectively [64]. Additionally, the peak appears appeared peaks at 1730,1626,1230,1080, and 790 cm^{-1}, respectively that confirms the presence of C=O stretching, vibration from carbonyl groups, C=C vibration from aromatic carbon, C–OH stretching vibrations, C–O vibrations from epoxy groups, and C–O vibration from alkoxy group in graphene [65–67]. Existence of C=O stretching, vibration from carbonyl groups, C=C vibration from aromatic carbon, C–OH stretching vibrations, C–O vibrations from epoxy groups, and C–O vibration from alkoxy group in graphene [65–67]. The spectrum of synthesized hybrid materials (CdS/Graphene) indicates the existence presence of C=C having moderate bonding at 1600 cm^{-1}, C=C bond having strong bond at 750 cm^{-1}, C–OH bond at 1350 cm^{-1}, C–O–C bond at 1230 cm^{-1}. Thus, the appearance of new peaks and shifting of peaks show the confirmation of the existence of interaction between graphene and CdS.

3.6. Electrical analysis

For electrical analysis, the 4-point probe conductivity measurements of as-prepared films with graphene, CdS/Graphene hybrid were performed using Current-Voltage (I-V) measurements (figure 8). The current-voltage (I-V) characteristics of the CdS/Graphene hybrid showed a semiconducting behavior. The voltage across the sample and the current flowing through it were measured using electrometers of type (Keithley- 2361). Transverse current-voltage measurement was also performed employing a high-precision source meter. Figure 8 and table 2 indicate that the current is increased in presence of graphene due to an increment in grain size which further reveals an improvement in crystallinity.

In comparison with CdS, the enhancement in the current of CdS/Graphene hybrid has been observed that confirms the generation of photo induced charge carriers, which can be explained in figure 8. Therefore, electrical conductivity is observed to increase due to the variance of charge carrier density and mobility as well as the crystallization of grains.

The electrical resistivity of CdS/Si, Graphene/Si, and CdS/Graphene/Si Thin films measured using the DC four-point probe technique. The resistivity follows the relation-

$$\rho = \frac{\pi}{\ln(2)} \times \left(\frac{V}{I}\right) = 4.532 \times \left(\frac{V}{I}\right)$$

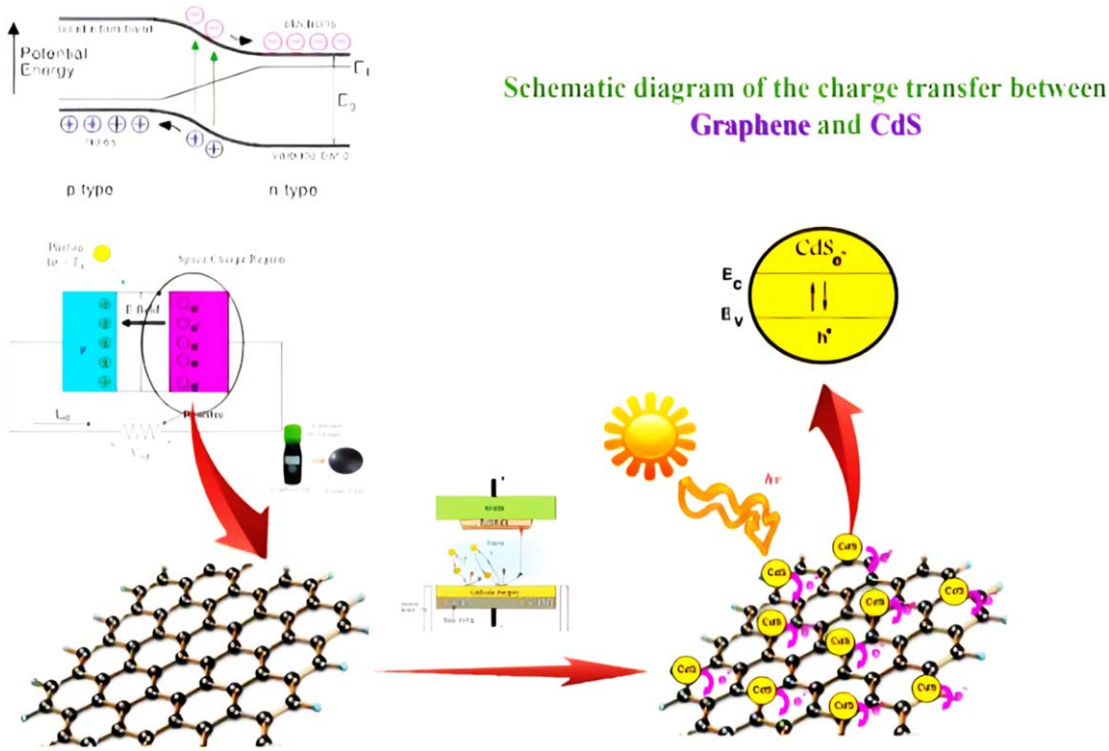

Figure 9. Schematic diagram of the charge separation and transfer in the Graphene– cadmium sulfide (Gr–CdS) system under visible light.

Table 2. Variation of sheet resistivity of CdS/Si, graphene/Si, and CdS/graphene/Si thin films.

Samples	CdS/Si	Graphene/Si	CdS/Graphene/Si
Sheet resistivity	350	6.5	3.4

3.7. MECHANISM/ THEOREM section-

The above analysis is based on the excitation mechanism of charge transfer. The physical and chemical properties of Cadmium sulfide (CdS) (II-VI semiconductor) are well known [68]. Which has a suitable band gap that could accelerate photo-induced electron transfer and electron-hole pair separation. A similar mechanism has been reported previously for TiO_2-graphene and ZnO-graphene composites [69, 70]. The schematic diagram of the charge transfer mechanism is shown briefly in figure 9. When CdS is exposed to visible light, it absorbed visible light considerably. Generation of photo-induced electron-hole has been taken place, which causes the appreciable enhancement of local EM-Field near the rough surface of CdS by photo-excited 'electrons' and 'holes'. It was previously reported that the electrons stored properties in CdS and charge transfer mechanism are readily scavenged by carbon nanomaterials such as graphene, fullerenes, and carbon nanotubes [71–73]. Additionally, because of physical and chemical properties i.e. high conductivity Graphene could promote charge separation and impede the electron-hole pair generation. The energy barrier between CdS and Graphene is about 1 eV. Therefore, Graphene acts as an electron acceptor in our system which was reported in previous studies [74, 75].

$$CdS + h\vartheta \rightarrow CdS(h + e)$$

$$CdS(e) + Graphene \rightarrow CdS/Graphene\ hybrid$$

In the present study, Graphene interacts with CdS undergo visible irradiation. The slow addition of Graphene with Cd^{2+} ion and S^{2-} ion provides uniform solubility, better adhesion, and maximum substitution of ion on the surface of Graphene sheets. Graphene has an excellent capability in capturing, storing the charge carriers and offers them to provide more opportunities to contact with a reactant in various photo-catalytic activities. Therefore, Graphene tends to enhance the availability and lifetime of charge carriers. Thus improve the photo catalytic and optoelectronic properties of CdS. Therefore, Graphene largely enhances the availability and lifetime of charge carriers, and thus improves the physical properties of CdS.

4. Conclusion

We proposed a simple and productive method for the hybridization of CdS nanospheres with graphene nanosheets to enhance photocurrent. A hybrid CdS/Graphene via RF sputtering method was synthesized. The electron exchange from energized CdS nanoparticles to graphene is effective in reducing the resistivity of graphene nanofilms.

Synthesized hybrid showed excellent optoelectronic properties and graphene has helped in the promotion of charge carrier, separation, and transfer, responsible for the aggregation and overgrowth of CdS and enhancing photocurrent, and improving the photo stability. The current-voltage characteristics of hybrid composite films appear straight linear behavior and the resistivity was observed to be decreased. Thus, synthesized hybrid is selective for the light source and can be utilized for various device applications including solar cells, biosensors like photo detector.

Acknowledgments

For the financial support of this study, the authors would like to thank the Department of Science and Technology (DST-SERB), India- CRG/2019/000903 (Core Research Grant) & SB/S2/RJN-140/2014 (Ramanujan Fellowship Award).

Data availability statement

All data that support the findings of this study are included within the article (and any supplementary files).

Conflict of interest

There are no conflicts to declare.

ORCID iDs

Zohreh Ghorannevis https://orcid.org/0000-0002-3692-7540
Avanish S Parmar https://orcid.org/0000-0003-1378-2438

References

[1] Yu W W and Peng X 2002 Formation of high-quality CdS and other II–VI semiconductor nanocrystals in noncoordinating solvents: tunable reactivity of monomers *Angew. Chem. Int. Ed.* **41** 2368–71
[2] Lei Y, Jiang Z and Zhang Z 2018 Effects of Zn/S ratios on the photoelectric properties of ZnS/microcrystalline graphene composites *J. Mater. Sci.: Mater. Electron.* **29** 7675–80
[3] Sang L, Liao M and Sumiya M 2013 A comprehensive review of semiconductor ultraviolet photodetectors: from thin film to one-dimensional nanostructures *Sensors* **13** 10482–518
[4] Omnès F *et al* 2007 *Wide bandgap UV photodetectors: A Short Review of Devices and Applications. Gallium Nitride Materials and Devices II Int. Society for Optics and Photonics*
[5] Bilgaiyan A *et al* 2015 *Improved Photoresponse of Hybrid ZnO/P3HT Bilayered Photodetector Obtained Through Oriented Growth of ZnO Nanorod Arrays and the Use of Hole Injection Layer J. Electron. Mater.* **44** 2842–8
[6] Sharma B K and Khare N 2013 Effect of UV exposure on rectifying behavior of polyaniline/ZnO heterojunction *Semicond. Sci. Technol.* **28** 125022
[7] Singh A K *et al* 2015 *Tailoring the electrical properties of multilayer MoS_2 transistors using ultraviolet light irradiation RSC Adv.* **5** 77014–8
[8] Gao Z *et al* 2012 Graphene–CdS composite, synthesis and enhanced photocatalytic activity *Appl. Surf. Sci.* **258** 2473–8
[9] Shyju T *et al* 2011 Solvothermal synthesis, deposition and characterization of cadmium selenide (CdSe) thin films by thermal evaporation technique *J. Cryst. Growth* **337** 38–45
[10] Leal-Cruz A *et al* 2014 Microstructural and optical characterizations of highly stable nanospheres of crystalline CdS via selective approach *Opt. Mater. Express* **4** 129–41
[11] Walker B *et al* 2014 Solution-processed CdS transistors with high electron mobility *RSC Adv.* **4** 3153–7
[12] Tedsana W, Tuntulani T and Ngeontae W 2013 A highly selective turn-on ATP fluorescence sensor based on unmodified cysteamine capped CdS quantum dots *Anal. Chim. Acta* **783** 65–73
[13] Kirovskaya I and Filatova T 2012 Adsorption and electrophysical properties of semiconductors of the InSb-CdS system *Russ. J. Phys. Chem.* A **86** 639–44
[14] Brown P, Takechi K and Kamat P V 2008 Single-walled carbon nanotube scaffolds for dye-sensitized solar cells *J. Phys. Chem.* C **112** 4776–82
[15] Green M *et al* 2019 Solar cell efficiency tables (version-54) *Prog. Photovolt. Res. Appl* **27** 565–75 (Wiley)
[16] Gautam M, Shi Z and Jayatissa A H 2017 Graphene films as transparent electrodes for photovoltaic devices based on cadmium sulfide thin films *Sol. Energy Mater. Sol. Cells* **163** 1–8

[17] Brown P and Kamat P V 2008 Quantum dot solar cells. electrophoretic deposition of CdSe− C60 composite films and capture of photogenerated electrons with n C60 cluster shell *J. Am. Chem. Soc.* **130** 8890–1
[18] Schaller R D, Agranovich V M and Klimov V I 2005 High-efficiency carrier multiplication through direct photogeneration of multi-excitons via virtual single-exciton states *Nat. Phys.* **1** 189–94
[19] Ellingson R J *et al* 2005 Highly efficient multiple exciton generation in colloidal PbSe and PbS quantum dots *Nano Lett.* **5** 865–71
[20] Jia L *et al* 2011 Highly durable N-doped graphene/CdS nanocomposites with enhanced photocatalytic hydrogen evolution from water under visible light irradiation *J. Phys. Chem.* C **115** 11466–73
[21] Zhang H and Zhu Y 2010 Significant visible photoactivity and antiphotocorrosion performance of CdS photocatalysts after monolayer polyaniline hybridization *J. Phys. Chem.* C **114** 5822–6
[22] Huang Q and Gao L 2004 Synthesis and characterization of CdS/multiwalled carbon nanotube heterojunctions *Nanotechnology* **15** 1855
[23] Wang H *et al* 2020 Layer-by-layer assembled synthesis of hollow yolk-shell CdS–graphene nanocomposites and their high photocatalytic activity and photostability *J. Nanopart. Res.* **22** 1–14
[24] Pan D *et al* 2010 Hydrothermal route for cutting graphene sheets into blue-luminescent graphene quantum dots *Adv. Mater.* **22** 734–8
[25] Zhang Z *et al* 2012 Graphene quantum dots: an emerging material for energy-related applications and beyond. *Energy Environ. Sci.* **5** 8869–90
[26] Li Y *et al* 2011 An electrochemical avenue to green-luminescent graphene quantum dots as potential electron-acceptors for photovoltaics *Adv. Mater.* **23** 776–80
[27] Pandey M and Balachandran M 2019 Green luminescence and irradiance properties of carbon dots cross-linked with polydimethylsiloxane *J. Phys. Chem.* C **123** 19835–43
[28] Bendavid L I, Atsango A O and Smith R W 2020 Interfacial properties of pure and doped CdS/graphene composites: CdS (0001)/graphene and a CdS/graphene bilayer *Comput. Mater. Sci.* **177** 109537
[29] Bradac C, Xu Z-Q and Aharonovich I 2021 Quantum energy and charge transfer at two-dimensional interfaces *Nano Lett.* **21** 1193–204
[30] Alhammadi S *et al* 2020 Performance of graphene–cds hybrid nanocomposite thin film for applications in Cu (In, Ga) Se2 solar cell and H2 production *Nanomaterials* **10** 245
[31] Chen F *et al* 2020 Efficient treament of organic pollutants over CdS/graphene composites photocatalysts *Appl. Surf. Sci.* **504** 144422
[32] Lei Y *et al* 2019 Synthesis of graphene quantum dots doped CdS composites for photoelectric properties *Mater. Res. Express* **6** 125608
[33] Veeramalai C P *et al* 2021 Fabrication of graphene: CdSe quantum dots/CdS nanorod heterojunction photodetector and role of graphene to enhance the photoresponsive characteristics *Nanotechnology* **32** 315204
[34] Liu B *et al* 2016 Effects of deposition temperature and CdCl2 annealing on the CdS thin films prepared by pulsed laser deposition *J. Alloys Compd.* **654** 333–9
[35] Slonopas A *et al* 2016 Growth mechanisms and their effects on the opto-electrical properties of CdS thin films prepared by chemical bath deposition *Mater. Sci. Semicond. Process.* **52** 24–31
[36] García L *et al* 2015 Laser sintering of magnesia with nanoparticles of iron oxide and aluminum oxide *Appl. Surf. Sci.* **336** 59–66
[37] Choi J W *et al* 2003 Stoichiometry, morphology and structure of CdS layers grown on InP (1 0 0) from atomic sulfur beam generated from H2S gas and thermally evaporated Cd using molecular beam epitaxy *J. Cryst. Growth* **255** 1–7
[38] White F *et al* 1979 Growth of CuInSe2 on CdS using molecular beam epitaxy *J. Appl. Phys.* **50** 544–5
[39] Yılmaz S 2015 The investigation of spray pyrolysis grown CdS thin films doped with flourine atoms *Appl. Surf. Sci.* **357** 873–9
[40] Yılmaz S *et al* 2015 Comparative studies of CdS, CdS: Al, CdS: Na and CdS:(Al–Na) thin films prepared by spray pyrolysis *Superlattices Microstruct.* **88** 299–307
[41] Tsai C *et al* 1996 Studies of grain size effects in rf sputtered CdS thin films *J. Appl. Phys.* **79** 9105–9
[42] Compaan A *et al* 1994 Rf sputtering of CdTE and CdS for thin film PV *AIP Conf. Proc.* (American Institute of Physics)
[43] Rondiya S *et al* 2017 Synthesis of CdS thin films at room temperature by RF-magnetron sputtering and study of its structural, electrical, optical and morphology properties *Thin Solid Films* **631** 41–9
[44] Dai C *et al* 1992 High orientation CdS thin films grown by pulsed laser and thermal evaporation *J. Vac. Sci. Technol.* A **10** 484–8
[45] Iacomi F *et al* 2007 Structural studies on some doped CdS thin films deposited by thermal evaporation *Thin Solid Films* **515** 6080–4
[46] Lee J-H and Lee D-J 2007 Effects of $CdCl_2$ treatment on the properties of CdS films prepared by rf magnetron sputtering *Thin Solid Films* **515** 6055–9
[47] moon B-S, Lee J-H and Jung H 2006 Comparative studies of the properties of CdS films deposited on different substrates by RF sputtering *Thin Solid Films* **511** 299–303
[48] Nayeri F D *et al* 2016 Dye decorated ZnO-NWs/CdS-NPs heterostructures for efficiency improvement of quantum dots sensitized solar cell *Superlattices Microstruct.* **91** 244–51
[49] Wendling Z *et al* 2014 A method for estimating sub-state consumption of delivered energy *Indiana University, Bloomington School of Public & Environmental Affairs Research* 1–7 Paper No. 2431356
[50] Zeng B, Liu W and Zeng W 2019 Simple and environmentally-friendly synthesis of graphene–CdS hierarchical nanospheres and their photocatalytic performance *J. Mater. Sci.: Mater. Electron.* **30** 3753–9
[51] Khan M E, Khan M M and Cho M H 2016 CdS-graphene nanocomposite for efficient visible-light-driven photocatalytic and photoelectrochemical applications *J. Colloid Interface Sci.* **482** 221–32
[52] Guan Y *et al* 2019 Enhanced photocatalytic activity of TiO_2/graphene by tailoring oxidation degrees of graphene oxide for gaseous mercury removal *Korean J. Chem. Eng.* **36** 115–25
[53] Wang J *et al* 2014 One-pot synthesis of CdS–reduced graphene oxide 3D composites with enhanced photocatalytic properties *Cryst. Eng. Comm.* **16** 399–405
[54] Liu J *et al* 2010 Self-assembling TiO_2 nanorods on large graphene oxide sheets at a two-phase interface and their anti-recombination in photocatalytic applications *Adv. Funct. Mater.* **20** 4175–81
[55] Shi J.-W. *et al* 2012 Low-temperature synthesis of CdS/TiO_2 composite photocatalysts: influence of synthetic procedure on photocatalytic activity under visible light *J. Mol. Catal. A: Chem.* **356** 53–60
[56] Peng T *et al* 2012 Enhanced photocatalytic hydrogen production over graphene oxide–cadmium sulfide nanocomposite under visible light irradiation *The J. Phys. Chem* C **116** 22720–6
[57] Ferrari A C and Robertson J 2000 Interpretation of Raman spectra of disordered and amorphous carbon *Phys. Rev.* B **61** 14095
[58] Graf D *et al* 2007 Spatially resolved Raman spectroscopy of single-and few-layer graphene *Nano Lett.* **7** 238–42
[59] Calizo I *et al* 2007 Temperature dependence of the Raman spectra of graphene and graphene multilayers *Nano Lett.* **7** 2645–9
[60] Elias D C *et al* 2009 Control of graphene's properties by reversible hydrogenation: evidence for graphane *Science* **323** 610–3
[61] Ghaemi F *et al* 2015 Few-and multi-layer graphene on carbon fibers: synthesis and application *RSC Adv.* **5** 81266–74

[62] Ferrari A C 2007 Raman spectroscopy of graphene and graphite: disorder, electron–phonon coupling, doping and nonadiabatic effects *Solid State Commun.* **143** 47–57
[63] Subrahmanyam K *et al* 2010 A study of graphene decorated with metal nanoparticles *Chem. Phys. Lett.* **497** 70–5
[64] Bose S *et al* 2012 Dual role of glycine as a chemical functionalizer and a reducing agent in the preparation of graphene: an environmentally friendly method *J. Mater. Chem.* **22** 9696–703
[65] Uddin M E *et al* 2015 Preparation of reduced graphene oxide-$NiFe_2O_4$ nanocomposites for the electrocatalytic oxidation of hydrazine *Composites Part B: Engineering.* **79** 649–59
[66] Bose S *et al* 2010 In-situ synthesis and characterization of electrically conductive polypyrrole/graphene nanocomposites *Polymer* **51** 5921–8
[67] Kumar A and Prakash R 2014 Graphene sheets modified with polyindole for electro-chemical detection of dopamine *J. Nanosci. Nanotechnol.* **14** 2501–6
[68] Zhang H *et al* 2014 SnO_2 nanoparticles-reduced graphene oxide nanocomposites for NO_2 sensing at low operating temperature *Sensors Actuators* B **190** 472–8
[69] Williams G and Kamat P V 2009 Graphene− semiconductor nanocomposites: excited-state interactions between ZnO nanoparticles and graphene oxide *Langmuir* **25** 13869–73
[70] Akhavan O 2011 Photocatalytic reduction of graphene oxides hybridized by ZnO nanoparticles in ethanol *Carbon* **49** 11–8
[71] Williams G, Seger B and Kamat P V 2008 TiO_2-graphene nanocomposites. UV-assisted photocatalytic reduction of graphene oxide *ACS Nano.* **2** 1487–91
[72] Kamat P V, Bedja I and Hotchandani S 1994 Photoinduced charge transfer between carbon and semiconductor clusters. One-electron reduction of C60 in colloidal TiO_2 semiconductor suspensions *J. Phys. Chem.* **98** 9137–42
[73] Kongkanand A and Kamat P V 2007 Electron storage in single wall carbon nanotubes. fermi level equilibration in semiconductor–SWCNT suspensions *ACS Nano.* **1** 13–21
[74] Deng Y *et al* 2019 A structural engineering-inspired CdS based composite for photocatalytic remediation of organic pollutant and hexavalent chromium *Catal. Today* **335** 101–9
[75] Qian J *et al* 2018 Tailoring the electronic properties of graphene quantum dots by P doping and their enhanced performance in metal-free composite photocatalyst *J. Phys. Chem.* C **122** 349–58